ChemMedChem

Chemistry Europe
European Chemical Societies Publishing

Accepted Article

Title: Synthesis, computational studies and assessment of in vitro inhibitory activity of squalene derivatives as carbonic anhydrase inhibitors.

Authors: andrea angeli, Lilia Clima, Bogdan Florin Craciun, Andrea Petreni, Alessandro Bonardi, Alessio Nocentini, Fabrizio Carta, Paola Gratteri, Mariana Pinteala, and Claudiu T. Supuran

To be cited as: *ChemMedChem* 10.1002/cmdc.202000500

Link to VoR: https://doi.org/10.1002/cmdc.202000500

WILEY-VCH

WILEY-VCH

FULL PAPER

Synthesis, computational studies and assessment of *in vitro* inhibitory activity of squalene derivatives as carbonic anhydrase inhibitors.

Lilia Clima,[a] Bogdan Florin Craciun,[a] Andrea Angeli,*[a,b] Andrea Petreni,[a,b] Alessandro Bonardi,[c] Alessio Nocentini,[c] Fabrizio Carta,[b] Paola Gratteri,[c] Mariana Pinteala,[a] Claudiu T. Supuran*[b]

[a] L. Clima, B.F.Craciun, A. Angeli, A. Petreni, M. Pinteala
Centre of Advanced Research in Bionanoconjugates and Biopolymers Department, "Petru Poni"
Institute of Macromolecular Chemistry,
700487 Iasi, Romania.
E-mail: andrea.angeli@unifi.it; claudiu.supuran@unifi.it

[b] A. Angeli, A. Petreni, F. Carta, C.T. Supuran
University of Florence
NEUROFARBA Dept., Sezione di Scienze Farmaceutiche,
Via Ugo Schiff 6, 50019 Sesto Fiorentino (Florence), Italy.

[c] A. Bonardi, A. Nocentini, P. Gratteri
University of Florence
Department of Neurosciences, Psychology, Drug Research and Child Health (NEUROFARBA), Section of Pharmaceutical and Nutraceutical Sciences,
Laboratory of Molecular Modeling Cheminformatics & QSAR
Via Ugo Schiff 6, 50019 Sesto Fiorentino (Florence), Italy.

Abstract: We report novel molecules incorporting the nontoxic squalene scaffold and different carbonic anhydrase inhibitors (CAIs). Potent inhibitory action, in the low nanomolar range, was detected against isoforms hCA II for sulfonamide derivatives, which proved to be selective against this isoform over the tumor-associate hCA IX and XII isoforms. On the other hand, coumarin derivatives showed weak potency but high selectivity against the tumor-associated isoform CA IX. These compounds are interesting candidates for preclinical evaluation in glaucoma or various tumors in which the two enzymes are involved. In addition, an *in silico* study of inhibitors bound hCA II revealed extensive interactions with the hydrophobic pocket of active site and provided molecular insights into the binding properties of these new inhibitors.

Introduction

Squalene is a unique 30-carbon, polyunsaturated hydrocarbon of the triterpene class, formed by six isoprene units which is widely in nature, from animals to plants (**Figure 1**). Since its discovery in 1903 in the shark liver extract, squalene has been investigated extensively and reported to play crucial roles in the steroid synthesis as a biochemical precursor of cholesterol and other steroids. [1]

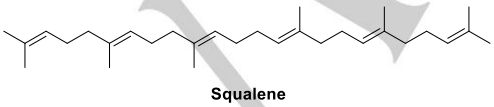

Figure 1: Chemical structures of squalene

In humans, squalene is synthesized in the liver and the skin, being transported in the blood by very low density lipoproteins (VLDL) and low density lipoproteins (LDL), and is secreted in large quantities by the sebaceous glands [2,3]. In the last years, the members of this class of terpenes gained considerable potential for drug and gene delivery applications.[4] In various studies, it was found that squalene effectively inhibits induced tumor genesis [5,6] and also efficiently improves the immune system [7,8] indicating its high potential for pharmaceutical and cosmetic applications.[9-11] Recently, it also gained much interest as drug carriers applications, for the effective transport of agents towards a targeted location or for keeping an effective agent unharmed in different conditions in the body. In this manner, squalene is a preferred agent due to its nontoxic nature and ability to form a protective vesicle and fuse the cell membrane easily [12,13]. In this context, our efforts have been focused on combining the nontoxic properties of squalene with different carbonic anhydrase inhibitors (CAIs) in order to decrease the possible side effects of these agents and also to generate hybrid compounds incorporating the two moeities. Carbonic anhydrases (CAs, EC 4.2.1.1) are ubiquitous metalloenzymes that catalyze the reversible hydration of carbon dioxide (CO_2) to generate bicarbonate anion (HCO_3^-) and a proton (H^+).[14,15] These proteins are present in most living organisms and are encoded by eight evolutionarily unrelated gene families: the α-, β-, γ-, δ-, ζ-, η-, θ-, and ι-CAs.[16-23] Human CAs (hCAs) all belong to the α-family and are present in 15 isoforms, which differ for tissue distribution, cellular localization, and kinetic properties. [24,25] The reaction catalyzed by these enzyme contributes to a range of physiological functions involved in different biological pathway, which among others include pH and bicarbonate homeostasis, respiration, bone metabolism and tumorigenesis.[24-28] In addition, their abnormal levels and/or activities often have been associated with different human diseases. Although in clinical use for decades, in the last years, CAs have become an interesting target for the design of inhibitors or activators with novel, non classical biomedical applications.[26,27,29] Indeed, CAIs were clinically used as diuretic,[30] antiglaucoma,[31] anticonvulsant,[32] or antiobesity agents[33] but more recently their use for the management of neuropathic pain and hypoxic tumors emerged.[34-36] The importance of modulating pH in the hypoxic tumor microenvironment underpins a strong case to develop innovative small-molecule inhibitors of CAs IX and XII for application as chemical probes. However, because of the large number of hCA isoforms, [14,15,24,25] there is a constant need

to improve the inhibition and selectivity profile of the so far developed CAIs, to avoid side effects due to inhibition of isoforms not involved in a certain pathology. In this study, we focused on new squalene compounds bearing the well know zinc binding group such as the sulfonamide and coumarin moieties. In particular we sought to make use of such an organic scaffold containing the sulfonamide moiety to improve the selectivity inhibition profile against the hCA II isoform, which is involved in several pathologies (i.e. glaucoma, epilepsy). In analogy the same strategy was considered for the coumarin containing series being particularly effective against the tumor associate isoforms hCA IX and XII.

Results and Discussion

Chemistry

CAI derivatives **8a-d** were synthesized following slightly modified literature procedures reported by our research group [37] and **Scheme 1** summarizes how the 6 and 7 coumarin derivatives (**4a-b**) were prepared. The synthesis started with protection of amine group of 1-bromoethyl-amine (**1**) and the key intermediates **3a**, **3b** were obtained by O-alkylation reaction between the commercially available 6-and 7-hydroxycoumarins (**2a**,**2b**) with the Boc-protected 1-bromoethyl-amine, followed by deprotection with trifluoroacetic acid (**4a**, **4b**).

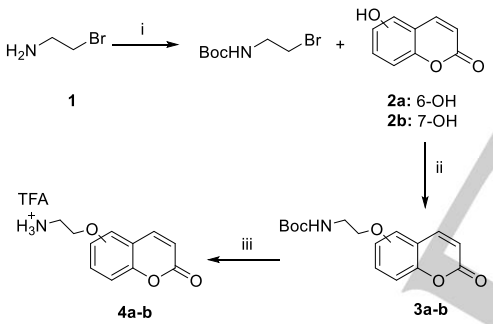

Scheme 1. Synthesis of the Key Intermediates **4a** and **4b**. i) $(Boc)_2O$ Et_3N DCM; ii) K_2CO_3 DMF 60°C iii) TFA, DCM..

Finally, the treatment of squalenic acid derivative **6** [38] with EDC-HCl and hydroxysuccinimide afford the corresponding active ester **7** that is reacted by nucleophic attack by amines **4a-b** and the commercially available sulphonamides **5a-b** using Et_3N as base to afford squalene amide derivatives **8a–d** as outlined in **scheme 2**.

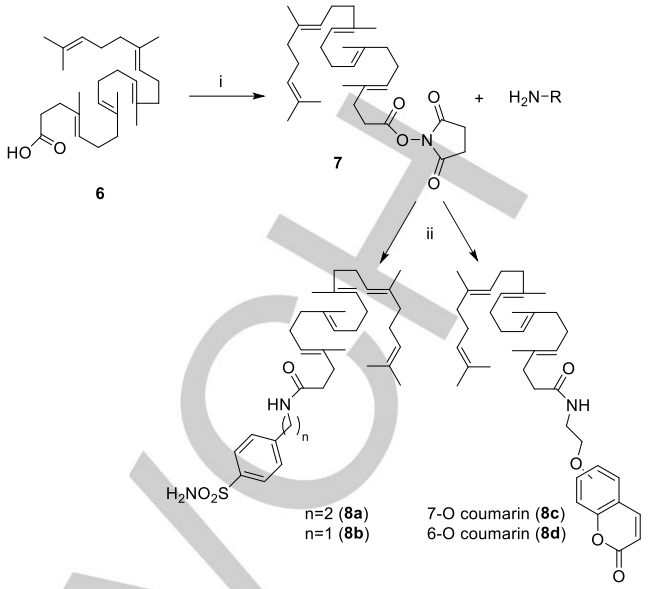

Scheme 2. Two steps synthesis pathway CAI-squalene derivatives. i) EDC-Cl, NHS, DMF dry, r.t. 2-4 h ii) Et_3N, DMF dry, 12-24 h r.t.

Carbonic anhydrase inhibition

All compounds **8a-d** were tested *in vitro* for their inhibitory activity against the physiologically relevant hCA isoforms I, II, IX and XII by means of the stopped-flow carbon dioxide hydration assay [39] and their activities were compared to the standard CAI acetazolamide (**AAZ**) (**Table 1**).

Table 1. nhibition data of human CA isoforms I, II, IX and XII with compounds **8a-d** and **AAZ** by a stopped flow CO_2 hydrase assay. [38]

	K_I (nM)[a]				
Cmp	**hCA I**	**hCAII**	**hCA IX**	**hCA XII**	**Selectivity ratio (CA II/IX)**
8a	3516	62.3	1887	844.0	0.0330
8b	6842	5.0	3559	>10000	0.0014
8c	>10000	>10000	7215	>10000	>1.386
8d	>10000	>10000	8817	>10000	>1.134
AAZ	250.0	12.1	25.8	5.7	0.468

[a] Mean from 3 different assays, by a stopped flow technique (errors were in the range of ± 5-10 % of the reported values).

Data of **Table 1** show the following interesting findings. The ubiquitous cytosolic isoform hCA I was poorly inhibited by sulphonamide derivatives **8a** and **8b** in micromolar range (3.5 and 6.8 µM, respectively). On the other hand, according to our previous reports, [37] compounds **8c** and **8d** did not inhibit the two cytosolic CAs, which is a desirable feature for compounds designed to target the tumor-associated enzymes. Sulfonamide derivatives **8a** and **8b** showed highly potency against hCA II with K_i of 62.3 and 5 nM with an high selectivity ratio for this isoform (0.033 and 0.0014, respectively). The tumor-associated isoform hCA XII was effectively inhibited only by compound **8a** in the range of high nanomolar (K_i 844.0 nM). Instead, the second tumor-associated isoform hCA IX was inhibited by all compounds here reported in the micromolar range and, in particular, compounds **8c** and **8d** showed selectivity inhibition against this isoform. Observations of selectivity ratios indicate the use of squalene tail shows the highest selectivity for the hCA II over the tumor isoforms with ratio of 30 II/IX for compound **8a** and over 710 fold for **8b**.

In silico studies

To correlate structural features and inhibition profiles of compounds **8a** and **8b**, docking and MM-GBSA-based refinements within CA II (PDB 5LJT)[39] active site were performed. In all docking solutions, the benzenesulfonamide scaffold accommodates deeply into the active site region, with the negatively charged nitrogen of zinc-binding group (SO_2NH^-) coordinating the metal atom (**Figure 2**). Additional H-bonds involving the zinc-binding group are established by the NH^- and S=O moieties of the sulfonamide with the side chain OH and backbone NH of T199, respectively. The phenyl ring accommodates within an area defined by V121, V143 and L198 (**Figure 2**). The aliphatic chains of compounds **8a** (**Figure 2A**) and **8b** (**Figure 2B**) spreads within the enzyme, forming stabilizing van der Waals contacts with the residues of the lipophilic half of the active site: I22, F131 V135, P202, and L204. In the case of **8a**, the squalene pendant reaches the region exposed to the solvent interacting with the surficial residues R27, P138, and E205, while not so for **8b** which thus is able to interact more extensively with the hydrophobic area involving, in addition, residues F20, P21, I91, and G132. Moreover, the shorter length of the methylamido (**8b**) over the ethylamidic (**8a**) linker makes the amide C=O of **8a** in H-bond distance with the Q92 side chain NH_2. It is likely that, together with the wider network of hydrophobic contact, this could explain the better inhibition profile of the methylamido vs ethylamido derivative.

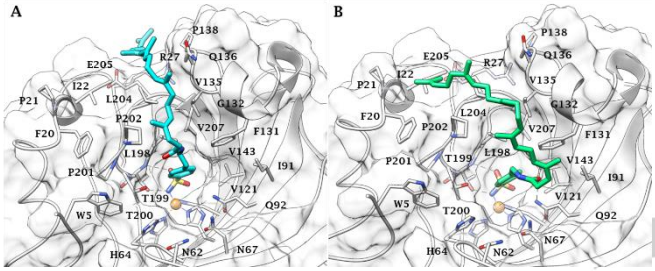

Figure 2. Predicted binding mode of compound (**A**) **8a** and (**B**) **8b** into CA II active site. H-bonds are represented as black dashed lines.

Conclusion

In conclusion, we synthetized a series of squalene-based carbonic anhydrase inhibitors by coupling reaction among squalenic acid derivative and different zinc binding groups such as sulphonamides and coumarin derivatives. The synthesized compounds were evaluated for the inhibition of isoforms hCA I, II, IX and XII, involved in a variety of diseases among which glaucoma, retinitis pigmentosa, tumors, etc. sulfonamide derivatives **8a** and **8b** showed highly selective and excellent inhibition profile of hCA II over the tumor-associate enzyme hCA IX and hCA XII. The effective inhibitory action against the cytosolic isoform hCA II making them interesting candidates for preclinical evaluation in glaucoma or related disease in which the hCA II is involved. Here we expand on these findings with novel information that, when coupled with our previous results, have allowed us to understand the key selective interactions designing linker regions of compounds with specific lengths to allow the compound's "tail" regions.

Experimental Section

General

All reactions were carried out in an oven-dried glassware under inert atmosphere (N_2). Ethanol was dried using a solvent purification system (Pure-Solv™). All commercial materials were used as received without further purification. Flash column chromatography purifications were performed with Silica gel 60 (230-400 mesh). Thin layer chromatography was performed with TLC plates Silica gel 60 F_{254}. NMR spectra were recorded in $CDCl_3$ or DMSO-d_6 with Mercury 400, and Bruker 400 Ultrashield spectrometers operating at 400 MHz (for ^{1}H), 100 MHz (for ^{13}C) and 376 MHz (for ^{19}F). NMR signals were referenced to nondeuterated residual solvent signals (7.26 and 2.50 ppm for ^{1}H, 77.0 and 40.5 ppm for ^{13}C). ^{1}H NMR data are reported as follows: chemical shift, integration, multiplicity (s = singlet, d = doublet, t = triplet, ap d = apparent doublet, m = multiplet, dd = doublet of doublet, bs = broad singlet, bd = broad doublet, ecc.), coupling constant (J), and assignment. The ESI-MS analysis was performed on an Agilent 6520 Series Accurate-Mass Quadrupole Time-of-Flight (Q-TOF) LC/MS equipment. Elemental composition of compounds was calculated on the basis of their measured accurate masses, accepting only results with an attribution error less than 5 ppm and a noninteger RDB (double-bond/ring equivalents) value. NMR and elemental composition analysis showed that the purity of all the final products was more than 95%.

General Procedure for the Synthesis of 2-((2-Oxo-2H-chromen-6-yl)oxy)ethan-1-ammonium Trifluoroacetate Salt 4a and 2-((2-Oxo-2H-chromen-7-yl)oxy)ethan-1-ammoniumTrifluoroacetate Salt 4b:

Step 1. Tert-Butyl (2-bromoethyl)carbamate (1.0 g, 1.0 equiv) was treated with 6-hydroxy-2H-chromen-2-one (6-OH) and K_2CO_3 (3.0equiv) in acetone or alternatively with 7-hydroxy-2H-chromen-2-one(7-OH) (1.0equiv) in the same conditions using dry DMF (5.0 mL) as solvent and under N_2 atmosphere. The reaction mixtures were stirred at 60°C overnight until consumption of starting materials (TLC monitoring), then cooled to room temperature and treated respectively as follows.

(i) The white precipitate was filtered off, and the obtained filtrate was concentrated under vacuum to afford the **3a** as an orange residue. (ii) The reaction was quenched with a 3.0 M aqueous hydrochloric acid solution to give a precipitate which was collected by filtration and triturated with diethyl ether to afford the 3b as a white solid.

Step 2. Tert-Butyl (2-((2-oxo-2H-chromen-6-yl)oxy)ethyl)carbamate **3a** (1.0 equiv) and tert-butyl (2-((2-oxo-2H-chromen-7-yl)oxy)ethyl)-carbamate **3b** (1.0 equiv) were dissolved in DCM, and TFA (6.0equiv) was added dropwise to the suspension. The solution was stirred at 0°C and then at room temperature until starting materials were consumed (TLC monitoring). The solvent was evaporated and the obtained residue dried under vacuo to afford the title compounds **4a** and **4b** as white solids.[37]

Synthesis of (4E,8E,12E,16E)-4,8,13,17,21-pentamethyl-N-(4-sulfamoylphenethyl)docosa-4,8,12,16,20-pentaenamide (8a):

Squalenic acid derivative **6** (0.4 g, 1 mmol, 1 equiv) was dissolved in 3 mL dry DMF under N_2 flow. EDC-HCl (0.288 g, 1.5 mmol, 1.5 equiv) and NHS (0.174 g, 1.5 mmol, 1.5 equiv) were solubilized in 2 mL dry DMF under N_2 flow and added dropwise to previously obtained derivative **6** solution under vigorous stirring. The mixture was stirred for 12h at room temperature (25 °C) until starting compounds consumed (TLC monitoring using 5% MeOH in DCM as eluent, not isolated). Obtained product in DMF solution (pale yellow) was used further as stock solution of derivative **7** with the concentration (82.95 mg/mL). To derivative **7** (75.75 mg, 0.05 mmol, 1 equiv), solution in dry DMF, Et_3N (101 µL, 0.75 mmol, 1.5 equiv) and 4-(2-aminoethyl)benzenesulphonamide (150 mg, 0.75 mmol, 1.5 equiv) were added and reaction mixture was stirred overnight at room temperature under N_2 flow. Next, water and HCl solution were added (pH ~3-4) and a solid compound precipitated. Crude product was washed with water and dried. Crude product was purified on silica gel column chromatography using ethyl acetate as eluent. Pure product **8a** was obtained as a yellow semisolid (yield: 243 mg, 83%) R_f = 0.8 (EtOAc). ^{1}H-NMR ($CDCl_3$, 400 MHz): 1.59 (15H, s, C*H*$_3$), 1.68 (3H, s, C*H*$_3$), 1.97-2.05 (16H, m, C*H*$_2$C*H*$_2$), 2.25 (4H, s, C*H*$_2$C*H*$_2$CO), 2.88 (2H, t, *J*=7.0 Hz, C*H*$_2$Ar), 3.50 (2H, m, C*H*$_2$NH), 4.97 (2H, s, N*H*2), 5.09-5.14 (5H, m, C*H*), 5.58 (1H, s, N*H*), 7.33 (2H, d, *J*=8.2 Hz, Ar*H*), 7.86 (2H, d, *J*=8.2 Hz, Ar*H*); ^{13}C-NMR (100 MHz, $CDCl_3$): 15.91, 16.02, 16.07, 17.68, 25.69, 26.70, 26.80, 28.28, 35.28, 35.74, 39.61, 39.74, 39.77, 40.30, 124.24, 124.27, 124.43, 124.51, 125.51, 126.80, 129.49, 131.27, 133.53, 134.89, 134.96, 135.23, 140.34, 144.52,

173.02. ESI-MS: Calculated for $C_{35}H_{54}N_2O_3S$ m/z: 582.39 (100.0%), found 583.5 [M+1]. Elemental Analysis: calculated C, 72.12; H, 9.34; N, 4.81; S, 5.50; found C, 72.10; H, 9.37; N, 4.80; S, 5.52.

Synthesis of (4E,8E,12E,16E)-4,8,13,17,21-pentamethyl-N-(4-sulfamoylbenzyl)docosa-4,8,12,16,20-pentaenamide (8b):

To derivate **7** solution in dry DMF (120 mg, 0.25 mmol, 1 equiv), Et_3N (108 µL, 0.75 mmol, 3 equiv) and 4-(aminomethyl)benzenesulfonamide hydrochloride (83.5 mg, 0.375 mmol, 1.5 equiv) were added and reaction mixture was stirred overnight at room temperature under N_2 flow. Next, water and HCl solution were added (pH ~3-4) and extracted with ethyl acetate. Organic layers were dried over Na_2SO_4, filtered and concentrated to dryness using vacuum. Crude product was purified on silica gel column chromatography using ethyl acetate as eluent. Pure product **8b** was obtained as a yellow semisolid (yield: 61.7 mg, 43%) R_f = 0.75 (EtOAc). ^{1}H-NMR ($CDCl_3$, 400 MHz): 1.59 (15H, s, C*H*$_3$), 1.67 (3H, s, C*H*$_3$), 1.92-2.08 (16H, m, C*H*$_2$C*H*$_2$), 2.31-2.31 (4H, m, C*H*$_2$C*H*$_2$CO), 4.42 (2H, d, *J*=6 Hz, C*H*$_2$NH), 5.07-5.18 (5H, m, C*H*), 5.31 (2H, s, N*H*$_2$), 6.37 (1H, t, J=6.0 Hz, N*H*), 7.29 (2H, d, *J*= 8.3 Hz, Ar*H*), 7.75 (2H, d, *J*= 8.3 Hz, Ar*H*); ^{13}C-NMR (100 MHz, $CDCl_3$): 15.93, 16.02, 16.08, 17.69, 25.70, 26.69, 26.74, 26.79, 28.28, 32.75, 34.40, 35.16, 35.29, 39.60, 39.74, 39.76, 42.84, 124.22, 124.25, 124.28, 124.41, 124.49, 125.30, 125.62, 126.63, 127.95, 131.25, 133.42, 134.89, 134.94, 135.21, 141.07, 143.72, 173.41, 177.20. ESI-MS: Calculated for $C_{34}H_{52}N_2O_3S$ m/z: 568.37 (100.0%), found 569.45 [M+1]. Elemental Analysis: calculated C, 71.79; H, 9.21; N, 4.92; S, 5.64; found C, 71.77; H, 9.23; N, 4.91; S, 5.65.

Synthesis of (4E,8E,12E,16E)-4,8,13,17,21-pentamethyl-N-(2-((2-oxo-2H-chromen-6-yl)oxy)ethyl)docosa-4,8,12,16,20-pentaenamide (8c):

Derivative **7** (0.039 g, 0.078 mmol, 1 equiv, 0.47 mL) was diluted with 7 mL dry DMF under N_2 flow. **4a** (0.038 g, 0.118 mmol, 1.5 equiv) and Et_3N (0.024 g, 0.235 mmol, 3 equiv) were solubilized in 3 mL dry DMF under N_2 flow and added dropwise over derivative **7** solution. The obtained mixture was stirred for 24h at room temperature under N_2 atmosphere until the starting products consumed. Obtained yellow solution was worked up as usually. The organic layers were washed with brine (2 x 30 mL), dried over Na_2SO_4, filtered off and concentrated to dryness under vacuum to give a yellow oil that was purified by silica gel column chromatography, eluting with an appropriate mixture of solvents (20% hexane in ethyl acetate to 100% ethyl acetate), affording **8c** as yellow semisolid (yield 0.0167g, **69%**) with $\mathbf{R_f}$ = 0.74 (ethyl acetate 100%). ^{1}H-NMR ($CDCl_3$, 400 MHz): 1.57-168 (18H, m, CH_3), 1.91-2.10 (16H, m, C*H*$_2$C*H*$_2$), 2.31 (4H, s, C*H*$_2$C*H*$_2$CO), 3.65-3.69 (2H, m, C*H*$_2$NH), 4.06 (2H t, *J* = 5.1 Hz, C*H*$_2$O), 5.03– 5.24 (5H, m, C*H*), 5.90-6.01 (1H, m, NH), 6.43 (1H d, *J* = 9.5 Hz, Ar*H*), 6.92 (1H, d, *J* = 2.6 Hz, Ar*H*), 7.10 (1H, dd, *J* = 9.0, 2.8 Hz, Ar*H*), 7.63 (1H, d, *J* = 9.6 Hz, Ar*H*); ^{13}C-NMR (100 MHz, $CDCl_3$): 16.51, 16.61, 16.63, 16.66, 18.28, 26.29, 27.28, 27.39, 28.87, 35.85, 35.87, 39.49, 40.20, 40.34, 40.36, 68.16, 111.36, 113.15, 117.90, 118.66, 119.87, 120.43, 124.81, 124.85, 125.01, 125.09, 126.18, 131.86, 134.05, 135.43, 135.55, 135.82, 143.65, 149.33, 155.60, 161.46, 173.85. ESI-MS: Calculated for $C_{38}H_{53}NO_4$ m/z: 587.40 (100.0%), found 588.51 [M+1]. Elemental Analysis: calculated C, 77.64; H, 9.09; N, 2.38; found C, 77.65; H, 9.10; N, 2.36.

Synthesis of (4E,8E,12E,16E)-4,8,13,17,21-pentamethyl-N-(2-((2-oxo-2H-chromen-7-yl)oxy)ethyl)docosa-4,8,12,16,20-pentaenamide (8d):

Derivative **7** (0.058 g, 0.116 mmol, 1 equiv, 0.7 mL) was diluted with 7 mL dry DMF under N_2 flow. Compound **4b** (0.056 g, 0.174 mmol, 1.5 equiv) and Et_3N (0.035 g, 0.35 mmol, 3 equiv) were solubilized in 3 mL dry DMF under N_2 flow and added dropwise over compound **7** solution. The obtained mixture was stirred for 24h at room temperature under N_2 atmosphere until the starting products consumed and the obtained yellow solution was worked up as usually. The organic layers were washed with brine (2 x 30 mL), dried over Na_2SO_4, filtered off and concentrated to dryness under vacuum to give a yellow oil that was purified by silica gel column chromatography, eluting with an appropriate mixture of solvents (20% hexane in ethyl acetate to 100% ethyl acetate), affording **8d** as yellow semisolid (yield 0.021g, **31%**) with R_f = 0.72 (ethyl acetate 100%). ^{1}H-NMR ($CDCl_3$, 400 MHz): 1.59 (15H, s, C*H*$_3$), 1.67 (3H, s, C*H*$_3$), 1.90-2.10 (16H, m, C*H*$_2$C*H*$_2$), 2.31 (4H, s, C*H*$_2$C*H*$_2$CO), 3.65-3.69 (2H, m, C*H*$_2$NH), 4.08 (2H, t, J=5.0 Hz, C*H*$_2$O), 5.01-5.26 (5H, m, C*H*), 5.98 (1H, s, NH), 6.26 (1H, d, J = 9.5 Hz, Ar*H*) ,6.80 (1H, d, J = 2.1 Hz, Ar*H*), 6.83 (1H, dd, J = 8.6, 2.3 Hz, Ar*H*), 7.38 (1H, d, J = 8.5 Hz, Ar*H*), 7.63 (1H, d, J = 9.5 Hz, Ar*H*); ^{13}C-NMR (100 MHz, $CDCl_3$): 16.51, 16.62, 18.28, 26.29, 27.28, 28.87, 35.83, 39.29, 40.19, 40.34, 68.13, 102.54, 112.83, 113.57, 114.14, 125.02, 129.53, 134.08, 143.81, 156.44, 161.59, 162.27, 173.68. ESI-MS: Calculated for $C_{38}H_{53}NO_4$ m/z: 587.40 (100.0%), found 588.48 [M+1]. Elemental Analysis: calculated C, 77.64; H, 9.09; N, 2.38; found C, 77.62; H, 9.12; N, 2.40.

Carbonic anhydrase inhibition

An Applied Photophysics stopped-flow instrument has been used for assaying the CA catalysed CO_2 hydration activity.[38] Phenol red (at a concentration of 0.2 mM) has been used as indicator, working at the absorbance maximum of 557 nm, with 20 mM Hepes (pH 7.5) as buffer, and 20 mM Na_2SO_4 (for maintaining constant the ionic strength), following the initial rates of the CA-catalyzed CO_2 hydration reaction for a period of 10–100 s. The CO_2 concentrations ranged from 1.7 to 17 mM for the determination of the kinetic parameters and inhibition constants. For each inhibitor at least six traces of the initial 5–10% of the reaction have been used for determining the initial velocity. The uncatalyzed rates were determined in the same manner and subtracted from the total observed rates. Stock solutions of inhibitor (0.1 mM) were prepared in distilled-deionized water and dilutions up to 0.01 nM were done thereafter with the assay buffer. Inhibitor and enzyme solutions were preincubated together for 15 min at room temperature prior to assay, in order to allow for the formation of the E-I complex. The inhibition constants were obtained by non-linear least-squares methods using PRISM 3 and the Cheng–Prusoff equation, as reported earlier,[40-42] and represent the mean from at least three different determinations. All CA isofoms were recombinant ones obtained in-house as reported earlier. [40-42]

Molecular modeling

The crystal structure of CA II (pdb 5LJT),[39] was prepared using the Protein Preparation Wizard tool implemented in Maestro - Schrodinger suite, assigning bond orders, adding hydrogens, deleting water molecules, and optimizing H-bonding networks[43]. Energy minimization protocol with a root mean square deviation (RMSD) value of 0.30 was applied using an Optimized Potentials for Liquid Simulation (OPLS3e) force field. 3D ligand structures were prepared by Maestro[43a] and evaluated for their ionization states at pH 7.4 ± 0.5 with Epik.[43b] OPLS3e force field in Macromodel[43c] was used for energy minimization for a maximum number of 2500 conjugate gradient iteration and setting a convergence criterion of 0.05 kcal $mol^{-1}Å^{-1}$. The docking grid was centered on the mass center of the co-crystallized ligands and Glide used with default settings. Ligands were docked with the standard precision mode (SP) of Glide[43c] and the best 5 poses of each molecule retained as output. The best pose for each compound, evaluated in terms of coordination, hydrogen bond interactions and hydrophobic contacts, was refined with Prime[43d] with a VSGB solvation model considering the target flexible within 3 Å around the ligand[44-46].

Acknowledgements

This work was supported by a grant of the Romanian Ministry of Research and Innovation, CNCS–UEFISCDI, project number PN-III-P4-ID-PCCF-2016–0050, within PNCDI II and project number PN-III-P1-1.1-TE-2016-1180, within PNCDI III..

Keywords: carbonic anhydrase; inhibitor, metalloenzymes, squalene, glaucoma

[1] B. Auffray *Int. J. Cosmet. Sci.* **2007**, 29, 23-29.
[2] P.V.I. Koivisto, T.A. Miettinen *Lipids* **1988**, 23, 993–996.
[3] M.E. Stewart *Semin. Dermatol.* **1992**, 11, 100–105.
[4] a) H. Relas, H. Gylling, T.A. Miettinen *J. Lipid Res.* **2001**, 42, 988–994. b) L. Clima, D. Peptanariu, M. Pinteala, A. Salic, M. Barboiu *Chem Commun (Camb).* **2015**, 51, 17529-17531. c) L. Clima, B.F. Craciun, G. Gavril, M. Pinteala *Polymers* **2019**, 11, 1313.
[5] A.L. Ronco, E.D. Stéfani *Funct. Foods Heal. Dis.* **2013**, 3, 462-476.
[6] W. Shi, M.N. Gould *Carcinogenesis* **2002**, 23, 131–142.
[7] E. Naziri, F. Mantzouridou, M.Z. Tsimidou *J. Agric. Food Chem.* **2011**, 59, 9980-9989.
[8] T. Ohkuma, K. O tagiri, S. Tanaka, T. Ikekawa *J. Pharmacobiodyn.* **1983**, 6, 148-151.
[9] S. Passi, O. De Pita, P. Puddu, G.P. Littarru *Free Radic. Res.* **2002**, 36, 471–477.
[10] B. Das, H. Yeger, H. Baruchel, M. Freedman, G. Koren, S. Baruchel *Eur. J. Cancer* **2003**, 39, 2556–2565.
[11] Kohno Y., Egawa Y., Itoh S., Nagaoka S., Takahashi M., Mukai K. *Biochim. Biophys. Acta* **1995**, 1256, 52–56.
[12] J.J. Wang, K. Sung, O.Y.P. Hu, C.H. Yeh, J.Y. Fang *J. Control. Release* **2006**, 115, 140–149.
[13] J.J. Wang, K. Sung, C.H. Yeh, J.Y. Fang *Int. J. Pharm.* **2008**, 353, 95–104.
[14] C.T. Supuran, C. Capasso *Metabolites.* 2017, 7, E56.
[15] Supuran C.T. *Expert Opin Drug Discov.* **2017**, 12, 61-88.
[16] C. Capasso, C.T. Supuran *Curr Med Chem.* **2015**, 22, 2130-2139.
[17] C. Capasso, C.T. Supuran *J Enzyme Inhib Med Chem.* **2015**, 30, 325-332.
[18] A. Angeli, M. Etxebeste-Mitxeltorena, C. Sanmartín, S. Espuelas, E. Moreno, A. Azqueta, S. Parkkila, F. Carta, C.T. Supuran *J Med Chem*. **2020**, 63, 4306-4314.
[19] A. Angeli, M. Pinteala, S.S. Maier, S. Del Prete, C. Capasso, B.C. Simionescu, C.T. Supuran *J Enzyme Inhib Med Chem*. **2019**, 34, 244-249.
[20] A. Angeli, M. Pinteala, S.S. Maier, S. Del Prete, C. Capasso, B.C. Simionescu, C.T. Supuran *J Enzyme Inhib Med Chem.* **2019**, 34, 644-650.
[21] A. Angeli, M. Buonanno, W.A. Donald, S.M. Monti, C.T. Supuran *Bioorg Chem.* 2018, 80, 261-265.
[22] A. Angeli, S. Del Prete, F.A.S. Alasmary, L.S. Alqahtani, Z. AlOthman, W.A. Donald, C. Capasso, C.T. Supuran *Bioorg Chem.* **2018**, 80, 94-98.
[23] E.L. Jensen, R. Clement, A. Kosta, S.C. Maberly, B. Gontero *ISME J.* **2019**, 13, 2094-2106.
[24] C.T. Supuran *Nat Rev Drug Discov.* **2008**, 7, 168-181.
[25] C.T. Supuran *Biochem J.* **2016**, 473, 2023-2032.
[26] C.T. Supuran, C. Capasso *Expert Opin Ther Pat.* **2018**, 28, 745-754.
[27] M. Bozdag, A.S.A. Altamimi, D. Vullo, C.T. Supuran, F. Carta *Curr Med Chem.* 2019, 26, 2558-2573.
[28] J.Y. Winum, M. Rami, A. Scozzafava, J.L. Montero, C.T. Supuran *Med Res Rev.* **2008**, 28, 3, 445-63.
[29] A. Angeli, F. Vaiano, F. Mari, E. Bertol, C.T. Supuran *J Enzyme Inhib Med Chem*. **2017**, 32, 1253-1259.
[30] F. Carta, C.T. Supuran *Expert Opin Ther Pat.* **2013**, 23, 681-691.
[31] C.T. Supuran, A.S.A. Altamimi, F. Carta Expert Opin Ther Pat. **2019**, 29, 781-792
[32] A. Di Fiore, G. De Simone, V. Alterio, V. Riccio, J.Y. Winum, F. Carta, C.T. Supuran *Org Biomol Chem.* **2016**, 14, 4853-4858.
[33] A. Scozzafava, C.T. Supuran, F. Carta *Expert Opin Ther Pat.* **2013**, 23, 725-35.
[34] C.T. Supuran *Expert Opin Investig Drugs.* **2018**, 27, 963-970.
[35] a) D. Tanini, L. Ricci, A. Capperucci, L. Di Cesare Mannelli, C. Ghelardini, T.S. Peat, F. Carta, A. Angeli, C.T. Supuran *Eur J Med Chem.* **2019**, 181, 111586. b) A. Angeli, M. Ferraroni, A. Nocentini, S. Selleri, P. Gratteri, C.T. Supuran, F. Carta *Chem Commun (Camb).* **2019**, 55, 5720-5723.
[36] S. Bua, L. Di Cesare Mannelli, D. Vullo, C. Ghelardini, G. Bartolucci, A. Scozzafava, C.T. Supuran, F. Carta *J Med Chem.* **2017**, 60, 1159-1170.
[37] A. Maksimenko, F. Dosio, J. Mougin, A. Ferrero, S. Wack, L.H. Reddy, A.-A. Weyn, E. Lepeltier, C. Bourgaux, B. Stella, L. Cattel, P. Couvreur *PNAS*, **2014**, 111, E217-226
[38] R.G. Khalifah *J. Biol. Chem*. **1971,** 246, 2561.
[39] J. Leitans, A. Kazaks, A. Balode, J. Ivanova, R. Zalubovskis, C.T. Supuran, K. Tars *J Med Chem*. **2015**, 58, 9004-9009
[40] A. Angeli, D. Tanini, A. Capperucci, G. Malevolti, F. Turco, M. Ferraroni, C.T. Supuran *Bioorg Chem.* **2018**, 81, 642-648.
[41] A. Angeli, L. Di Cesare Mannelli, E. Lucarini, T.S. Peat, C. Ghelardini, C.T. Supuran *Eur J Med Chem.* **2018** , 154, 210-219.
[42] A. Mocan, S. Carradori, M. Locatelli, D. Secci, S. Cesa, A. Mollica, S. Riga, A. Angeli, C.T. Supuran, C. Celia, L. Di Marzio *Food Chem Toxicol.* **2018**, 112, 441-447.
[43] Schrodinger Suite Release 2019-1, Schrodinger, LLC, New York, NY, 2019: (a) Prime, v.5.5; Maestro v.11.9; (b) Epik, v.4.7; (c) Glide, v.8.2; (d) Macromodel v.12.3.
[44] a) A. Nocentini, P. Gratteri, C.T. Supuran *Chemistry.* **2019**, 25, 1188-1192. b) C.T. Supuran *J Enzyme Inhib Med Chem.* **2018**, 33, 485-495.
[45] A. Nocentini, A. Bonardi, P. Gratteri, B. Cerra, A. Gioiello, C.T. Supuran *J Enzyme Inhib Med Chem.* **2018**, 33, 1453-1459.
[46] A. Nocentini, F. Carta, M. Tanc, S. Selleri, C.T. Supuran, C. Bazzicalupi, P. Gratteri *Chemistry.* **2018**, 24, 7840-7844

Entry for the Table of Contents

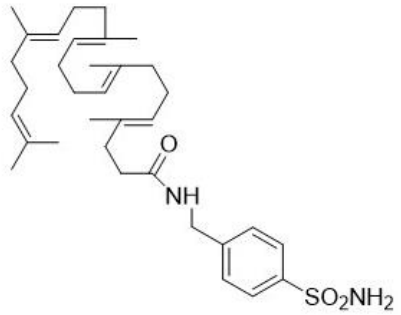

hCA II: 5.0 nM Vs hCA IX: 3559 nM